J. Fluid Mech. (2016), *vol.* 787, *pp.* 1–15.
doi:10.1017/jfm.2015.662

Internal hydraulic jumps in two-layer systems

Peter G. Baines†

Department of Infrastructure Engineering, University of Melbourne, Melbourne 3010, Australia

(Received 22 April 2015; revised 6 August 2015; accepted 3 November 2015;
first published online 7 December 2015)

This paper describes a new model of internal hydraulic jumps in two-layer systems that places no restrictions (such as the Boussinesq approximation) on the densities of the two fluids. The model is based on that of Borden and Meiburg (*J. Fluid Mech.*, vol. 276, 2013, R1) for Boussinesq jumps, and has the appropriate behaviour in various limits (single-layer, small amplitude, Boussinesq, infinite depth). The energy flux loss in each layer across the jump is positive for all realistic jumps, reaching a maximum for the jump with maximum speed. Larger-amplitude jumps are possible, with decreasing energy loss, down to the 'conjugate state' of zero energy loss. However, it is argued that such states may be difficult to realise in practice, and if formed, will tend to the jump with maximum speed. The energy loss is mostly in the contracting layer unless the density there is small. The two-layer model is extended to incorporate mixing between the layers within the jump, with mixing based on the Richardson number.

Key words: geophysical and geological flows, hydraulics, stratified flows

1. Introduction

As defined in this paper, hydraulic jumps (or bores – the two terms are equivalent and used interchangeably here) in two-layer fluids are flow structures that are, in effect, a transition between two steady two-layer flow states, each consisting of two layers with uniform velocity and density in each layer. Waves may propagate on the interface between the layers, but the upper and lower boundaries are rigid. The properties of the jump are defined by the properties of these two flows. In the cases considered here, in one of these flows (designated the upstream flow), the velocities of the two layers are the same, so that in the reference frame of this fluid, the jump is moving into (or conceivably away from) fluid at rest. The processes that are involved in this transition are not considered. Such hydraulic jumps may be turbulent and occupy a limited horizontal space, or they may involve a steady downstream wave train that causes a loss of energy flux downstream of the leading edge of the jump, which is ultimately dissipated by friction. In such circumstances, the downstream flow as defined by the jump is downstream of all this, though a good approximation of this downstream state may be obtained by taking the mean of the amplitude of the downstream wave.

The study of the dynamics of internal hydraulic jumps has a long history, commencing with the work of Yih & Guha (1955), who developed an analytical

† Email address for correspondence: p.baines@unimelb.edu.au

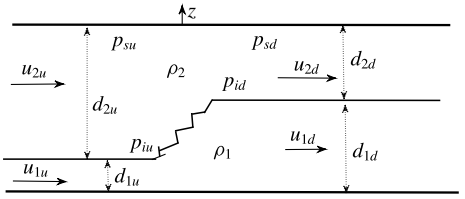

FIGURE 1. Schematic diagram with notation for the model of a two-layer hydraulic jump between two uniform states of motion. p_{su}, p_{sd}, p_{iu}, p_{id} denote the pressures at the upper surface and the interface upstream and downstream respectively, and velocities denote speeds in a frame of reference moving with the bore.

two-layer model that required the assumption that the flow within the jump be effectively hydrostatic. Since then, as a result of various laboratory experiments and numerical studies, a succession of different analytical models have been derived, though the most recent (and most accurate) models have been restricted by the requirement to make the Boussinesq approximation, implying that the difference between the densities of the two fluids involved must be very small.

In this paper, a model is presented that removes this restriction, and is applicable to two-layer fluids of all stable densities. In the next section the history of models of two-layer jumps is summarised, culminating in the model of Borden and Meiburg for Boussinesq fluids. It is then shown how the procedure that they used can be extended to the non-Boussinesq case, and that the resulting bore structure has all the appropriate features in terms of energy flux losses and various limits. In particular, for given initial conditions, as the jump amplitude is increased it reaches a maximum speed, which coincides with maximum energy flux loss in each layer; for larger amplitude the speed and energy flux losses decrease. It is argued that these flows with amplitudes beyond the jump of maximum speed, if they can be generated, are likely to be transient, unstable structures. The model is also extended to include mixing at the interface, creating a transition layer downstream, and some results are presented.

The approach here may be contrasted with that of Thorpe (2010) and Thorpe & Li (2014). The present model takes the simplest possible configuration of hydraulic jumps in stratified (two-layer) flow, and aims to obtain the correct solution for these conditions. From this point, generalisations that include mixing can be made, as is done in § 5. Thorpe's approach, on the other hand, is to make a different set of assumptions that include mixing processes and give results that are more complex but are more immediately applicable to realistic flows. One may anticipate some convergence between these two approaches.

2. A brief history of models of two-layer hydraulic jumps

The principal objective is to obtain an expression for the speed of a hydraulic jump between two two-layer flows in terms of its amplitude. Certain conditions are assumed, namely (1) the jump is steady in a reference frame moving with it, (2) the top and bottom surfaces are horizontal through the jump, with no surface stress, and (3) the layers maintain their identity through the jump, with negligible exchange of fluid between them. The conventional picture of a two-layer hydraulic jump is given in figure 1, with two flowing layers with densities ρ_1 and ρ_2. These densities may have any value, the only restriction being that $\rho_2 < \rho_1$. The flow has a rigid upper boundary with uniform total depth D, and the jump may be regarded as an essentially

turbulent structure (which dissipates energy) between a supercritical upstream flow state (in which waves cannot propagate upstream, away from the bore) with layer velocities u_{1u}, u_{2u} and thicknesses d_{1u}, d_{2u}, and a downstream state with velocities u_{1d}, u_{2d} and thicknesses d_{1d}, d_{2d} (which may be sub- or supercritical, as discussed in § 4). In principle the upstream flow may have any profile, but the upstream layer velocities are assumed to be the same in all cases considered here. Assuming that these flows are steady in the frame of the jump, we have

$$d_{1d} + d_{2d} = D = d_{1u} + d_{2u}, \quad d_{id}u_{id} = q_i = d_{iu}u_{iu}, \quad i = 1, 2, \tag{2.1a,b}$$

where q_i denotes the volume flux in the ith layer. From assumption (2) we also have that the momentum flux S must be uniform, so that

$$S = \int_0^D p + \rho u^2 \, \mathrm{d}z = \text{constant} \tag{2.2}$$

(where p denotes pressure), which implies

$$\begin{aligned} S &= p_{su}D + \tfrac{1}{2}\Delta\rho g d_{1u}^2 + \rho_1 u_{1u}^2 d_{1u} + \rho_2 u_{2u}^2 d_{2u} + \tfrac{1}{2}\rho_2 g D^2 \\ &= p_{sd}D + \tfrac{1}{2}\Delta\rho g d_{1d}^2 + \rho_1 u_{1d}^2 d_{1d} + \rho_2 u_{2d}^2 d_{2d} + \tfrac{1}{2}\rho_2 g D^2. \end{aligned} \tag{2.3}$$

This equation introduces an additional variable, $p_{su} - p_{sd}$, which needs to be determined by other considerations. The first attempt at this was by Yih & Guha (1955), who made the following three additional assumptions about the dynamics within the jump: (i) interfacial stresses are negligible, (ii) the flow is effectively hydrostatic, and (iii) the surface pressure p_s varies linearly with upper layer thickness d_2. These assumptions lead directly to the relation (Yih & Guha 1955; Baines 1995)

$$p_{su} - p_{sd} = 2\rho_2(d_{2d}u_{2d}^2 - d_{2u}u_{2u}^2)/(d_{2d} + d_{2u}). \tag{2.4}$$

Writing

$$r_u = d_{1u}/D, \quad r_d = d_{1d}/D, \tag{2.5a,b}$$

and $g' = \Delta\rho/\rho_1 g = ((\rho_1 - \rho_2)/\rho_1)g$, for the jump speed c_J equations (2.1)–(2.5) give

$$\frac{c_J^2}{g'D} = \frac{(r_u + r_d)/2}{\left[\dfrac{r_u}{r_d} + \dfrac{\rho_2}{\rho_1}\dfrac{(1 - r_u)(r_u + r_d)}{(1 - r_d)(2 - r_u - r_d)}\right]}. \quad \text{(YG)} \tag{2.6}$$

Subsequently, instead of assumptions (ii) and (iii) above, Chu & Baddour (1977) and Wood & Simpson (1984) made the assumption that all of the energy dissipation within the jump occurred in the expanding layer (the lower layer in figure 1). For Wood and Simpson this was suggested (to them) by their experiments, and it implies that the Bernoulli equation may be applied to the contracting layer. If this is the upper layer, it implies

$$p_{su} - p_{sd} = \tfrac{1}{2}\rho_2(u_{2d}^2 - u_{2u}^2), \tag{2.7}$$

and if it is the lower layer, it is

$$p_{su} - p_{sd} = \tfrac{1}{2}\rho_1(u_{1d}^2 - u_{1u}^2) + \Delta\rho g(d_{1d} - d_{1u}). \tag{2.8}$$

Using (2.7), with the configuration of figure 1 this gives

$$\frac{c_J^2}{g'D} = \frac{(r_u + r_d)/2}{\left[\dfrac{r_u}{r_d} + \dfrac{\rho_2}{\rho_1}\dfrac{r_u + r_d - 2r_u r_d}{2(1-r_d)^2}\right]}. \quad \text{(WS)} \tag{2.9}$$

The resulting bore speeds between these two expressions are similar unless the amplitudes are close to the maximum possible.

More recently, Klemp, Rotunno & Skamarock (1997) have made the opposite assumption to that of Wood and Simpson, namely that all of the dissipation occurs in the contracting layer, at least in the case of a Boussinesq fluid (where the densities are effectively equal except when multiplied by g). This is approximately consistent with their own numerical simulations, and with the assumptions of Benjamin (1968) regarding gravity currents. In the context of figure 1, this implies using (2.8) instead of (2.6) or (2.7), giving, for the full density range,

$$\frac{c_J^2}{g'D} = \frac{[1-(r_u+r_d)/2](1-r_d)r_d^2}{(1-r_d)[(r_d+r_u)/2 - r_u r_d] + \dfrac{\rho_2}{\rho_1} r_d^2(1-r_u)}. \quad \text{(KRS)} \tag{2.10}$$

The models are only applicable in situations where hydraulic jumps exist: generally for $r_u < 0.5$ and a limited range of $r_d > r_u$. These three models give different answers, particularly for small r_u. The YG and WS models give similar results but diverge at large amplitude, with YG the larger. The KRS model gives significantly lower jump speeds than both, but is believed to be more realistic, at least near the Boussinesq limit.

From the viewpoint of energy dissipation, there is something wrong with each of these models. An examination of the YG solution (2.6) shows that there is a net gain in energy flux in the upper (contracting) layer across the jump (Li & Cummins 1998), which would seem unphysical. For the other two models, an absence of energy loss in either layer also cannot be correct in general terms. A numerical study by Borden, Meiburg & Constantinescu (2012) of conditions in the Boussinesq limit showed that mixing at the interface could cause a gain of potential energy in the expanding (lower) layer, and they proposed a new model in this limit that involved the Reynolds and Schmidt numbers, which they denote as the BMC model.

3. Models based on vorticity generation

Subsequent to all of the above, Borden & Meiburg (2013) proposed a new method of solving the problem of the unknown surface pressure change across the jump. By making the Boussinesq approximation, they could write the two-dimensional vorticity equation for steady flow of incompressible fluids as

$$\boldsymbol{u}\cdot\nabla\omega = -g'\frac{\partial \rho^*}{\partial x} + \nu\nabla^2\omega, \tag{3.1}$$

where ω is the vorticity in the y-direction, $\rho^* = (\rho(z) - \rho_2)/(\rho_1 - \rho_2)$ and the pressure term does not appear. By integrating this vorticity equation in a control volume of fluid that includes the jump, and then employing the Gauss divergence theorem, they were able to obtain an equation for the vorticity generation within the jump, which provides a new equation linking upstream and downstream conditions. This provides

a new expression for the jump speed in the Boussinesq limit, which Borden and Meiburg term the vortex sheet (VS) model. It is shown here (and this is the central point of this paper) that this procedure may be extended to all density ratios, providing (in particular) a general relation for internal hydraulic jump speeds, as follows.

In general, the steady-state form of the vorticity equation (in the frame of the jump) has the form

$$\boldsymbol{u}\cdot\nabla\omega=\frac{1}{\rho^2}\nabla\rho\times\nabla p=-\nabla\times\left(\frac{1}{\rho}\nabla p\right). \tag{3.2}$$

We assume that the flow is on a sufficiently large scale so that the viscous term may be neglected. Since the fluids are incompressible so that $\nabla\cdot\boldsymbol{u}=0$, if (3.2) is integrated over the region of the jump (as represented in figure 1) one obtains for the left-hand side

$$\int_A \boldsymbol{u}\cdot\nabla\omega\,\mathrm{d}A=\int_A\nabla\cdot(\omega\boldsymbol{u})\,\mathrm{d}x\,\mathrm{d}z=\int\omega\boldsymbol{u}\cdot\mathrm{d}\boldsymbol{S}, \tag{3.3}$$

where area A is the region containing the jump as depicted in figure 1, and $\boldsymbol{S}$ denotes the boundary surfaces of A upstream and downstream. The last term of (3.3) denotes the flux of vorticity across surface $\boldsymbol{S}$. For jumps moving into stationary fluid, or fluid in uniform motion, there is no upstream vorticity. On the downstream side the vorticity is concentrated in the vortex sheet between the two fluids, and the flux of it is given by the vortex sheet strength times the mean velocity of the sheet, which is (Saffman 1992; Borden & Meiburg 2013)

$$\int\omega\boldsymbol{u}\cdot\mathrm{d}\boldsymbol{S}=-(u_{2d}-u_{1d})(u_{2d}+u_{1d})/2=-\frac{1}{2}(u_{2d}^2-u_{1d}^2). \tag{3.4}$$

The area integral of the right-hand side of (3.2) may be reduced by Stokes's theorem to a line integral around the boundary of area A enclosing the jump

$$-\int_A\nabla\times\left(\frac{1}{\rho}\nabla p\right)\mathrm{d}A=-\int\left(\frac{1}{\rho}\nabla p\right)\cdot\mathrm{d}\boldsymbol{l}, \tag{3.5}$$

in the anticlockwise sense. Since the density is uniform in each layer, the integral reduces to

$$-\int\left(\frac{1}{\rho}\nabla p\right)\cdot\mathrm{d}\boldsymbol{l}=\left(\frac{1}{\rho_2}-\frac{1}{\rho_1}\right)(p_{iu}-p_{id}), \tag{3.6}$$

where p_{iu} and p_{id} denote the upstream and downstream pressures at the interface respectively (see figure 1).

The upstream pressure at the interface is equal to $p_{su}+g\rho_2(D-d_{1u})$ and the corresponding downstream pressure is $p_{sd}+g\rho_2(D-d_{1d})$. Putting these terms into (3.6) and equating it with (3.4) gives

$$\frac{1}{2}(u_{2d}^2-u_{1d}^2)=\left(\frac{1}{\rho_2}-\frac{1}{\rho_1}\right)[p_{su}-p_{sd}+\rho_2 g(d_{1d}-d_{1u})]=\frac{\Delta\rho}{\rho_1}\frac{p_{su}-p_{sd}}{\rho_2}+g'(d_{1d}-d_{1u}). \tag{3.7}$$

This is the same expression as that derived by Borden and Meiburg, except that it has the additional term containing the difference in surface pressure, which would be discarded in taking the Boussinesq approximation. For previous models the difference in surface pressure was an unknown quantity, but (3.7) provides a value for it that may be combined with the value obtained from the conservation of momentum flux S

in (2.4). Eliminating $p_{su} - p_{sd}$ from these two equations gives the expression for the jump speed c_J (which in present notation is equal to u_{1u} and u_{2u}) in terms of its amplitude, which takes the form

$$\frac{c_J^2}{g'D} = \frac{r_d^2(1-r_d)^2\left[1+\left(\dfrac{\rho_1}{\rho_2}-1\right)\dfrac{r_d+r_u}{2}\right]}{\left[\dfrac{r_d+r_u}{2}-r_ur_d+\left(\dfrac{\rho_1}{\rho_2}-1\right)r_ur_d(1-r_d)^2-\left(1-\dfrac{\rho_2}{\rho_1}\right)r_d^2(1-r_u)(1-r_d)\right]}. \tag{3.8}$$

This model may be termed the 'full vortex sheet (FVS)' model. If $\rho_2 = \rho_1$ in this expression, giving the Boussinesq limit, it reduces to (2.9) of Borden and Meiburg for their 'vortex sheet (VS)' model. It also satisfies other required limits, as follows.

$$\text{If } r_d \to r_u\text{:} \quad c_J^2 \to c_0^2 \equiv \frac{\Delta\rho g}{\dfrac{\rho_1}{d_{1u}}+\dfrac{\rho_2}{d_{2u}}}, \tag{3.9}$$

where c_0 is the linear long-wave speed.

$$\text{If } \rho_2 \to 0\text{:} \quad c_J^2 \to \frac{gd_{1d}}{2}\left(1+\frac{d_{1d}}{d_{1u}}\right), \tag{3.10}$$

which is Rayleigh's relation for single-layer jumps (see Baines 1995, § 2.3.1).

$$\text{If } D \to \infty\text{:} \quad c_J^2 \to \frac{2g'd_{1d}^2}{d_{1u}+d_{1d}}. \tag{3.11}$$

None of the previous models (YG, WS and KRS) listed in § 2 conforms with all of these limits.

For some purposes it useful to compare the jump speed with the linear wave speed c_0 in (3.9), and (3.8) then becomes

$$\frac{c_J^2}{c_0^2} = \frac{r_d^2(1-r_d)^2\left[1-r_u\left(1-\dfrac{\rho_2}{\rho_1}\right)\right]\left[1+\left(\dfrac{\rho_1}{\rho_2}-1\right)\dfrac{r_d+r_u}{2}\right]}{r_u(1-r_u)\left[\dfrac{r_d+r_u}{2}-r_ur_d+\left(\dfrac{\rho_1}{\rho_2}-1\right)r_ur_d(1-r_d)^2-\left(1-\dfrac{\rho_2}{\rho_1}\right)r_d^2(1-r_u)(1-r_d)\right]}. \tag{3.12}$$

Some representative results for wave speeds from this model up to the point of maximum speed are shown in figure 2 for a range of density ratios, for $r_u = 0.1$, 0.2 and 0.35. For $\rho_2/\rho_1 = 0.99$ the results are very similar to those from the Boussinesq model of Borden and Meiburg and the KRS model. For $\rho_2/\rho_1 = 0.79$ the results may be compared with the observations of Baines (1984) with water and kerosene. Comparisons are shown in figure 3 for $r = r_u = 0.035$, 0.1 and 0.2, which give a reasonable fit to the data, significantly better than those with the model of Yih and Guha, with which the comparisons were presented in 1984.

The upper limit of r_u values for which upward jumps may occur is 0.5 for the Boussinesq limit, which is also observed numerically for $\rho_2/\rho_1 = 0.99$. However, for smaller values of ρ_2/ρ_1 this limit increases, and it reaches 0.75 for $\rho_2/\rho_1 = 0.1$. As the upper layer density vanishes, jumps (of modest sizes) are possible for r_u values approaching unity. Downward hydraulic drops are possible for r_u values ranging from 0.5 to 1 in the Boussinesq limit (and $\rho_2/\rho_1 = 0.99$), but as ρ_2/ρ_1 decreases the range shortens, to 0.54:1 for $\rho_2/\rho_1 = 0.79$, 0.765:1 for $\rho_2/\rho_1 = 0.1$, and it vanishes as $\rho_2/\rho_1 \to 0$.

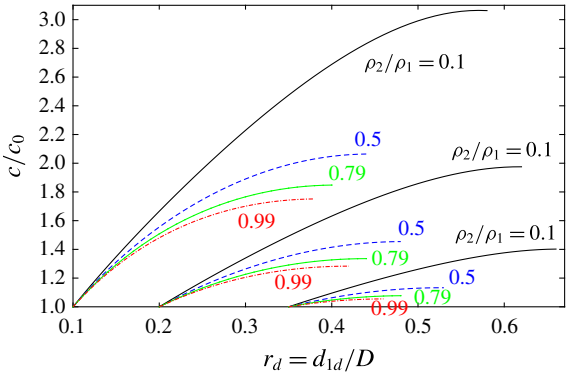

FIGURE 2. (Colour online) Hydraulic jump speeds c_J for the FVS model, for $\rho_2/\rho_1 = 0.1$, 0.5, 0.79 and 0.99 as a function of amplitude $r_d = d_{1d}/D$ for initial layer thickness $r_u = d_{1u}/D$ (given by the starting value of r_d). c_J has been scaled with the linear wave speed c_0.

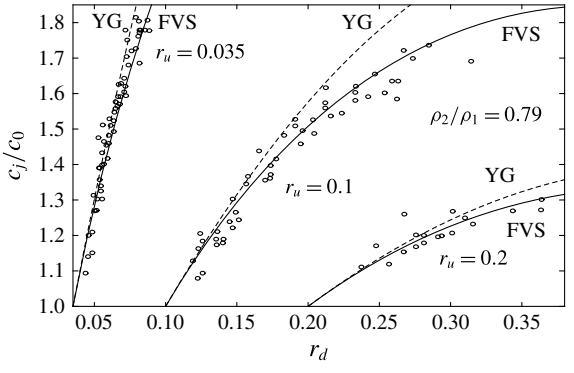

FIGURE 3. FVS model jump speeds for $r_u = 0.035$, 0.1 and 0.2 compared with experimental observations from Baines (1984) made with water and kerosene ($\rho_2/\rho_1 = 0.79$). The results obtained with the Yih–Guha (YG) model are also shown, and the FVS model is clearly a better fit.

4. Jump amplitudes, speeds and energy losses

The results shown in figure 2 have been terminated at the point of maximum speed of the hydraulic jumps. This is not the limit of the formal solutions for such jumps, as the solutions continue for larger amplitude, but at decreasing jump speed. These solutions are theoretically possible, but have lesser significance for two reasons, as given below. Examples are shown in figure 4 for $r_u = 0.035$ and 0.2, and in figure 5 for $r_u = 0.965$, 0.9, 0.8 and 0.65, where the jumps are downward (sometimes known as 'hydraulic drops'). In these figures the extensions at larger amplitude and lower speed beyond the point of maximum speed are shown as dashed. Figure 6 shows the losses in the energy flux in each layer for $r_u = 0.035$, 0.2, 0.8 and 0.965. Here one notes that the energy flux loss in each layer is everywhere positive, that both rise to a maximum at a common point, and then decrease to zero, again terminating at a common point.

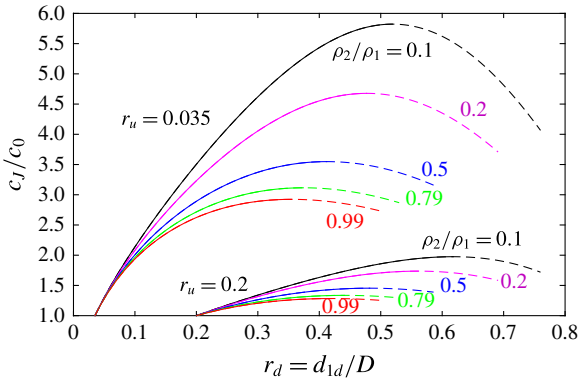

FIGURE 4. (Colour online) Hydraulic jump speeds c_J scaled with c_0 as in figure 2 but for the full range to the point of zero energy loss, for $r_u = 0.035$ and 0.2. Amplitudes greater than those for maximum speed are shown dashed.

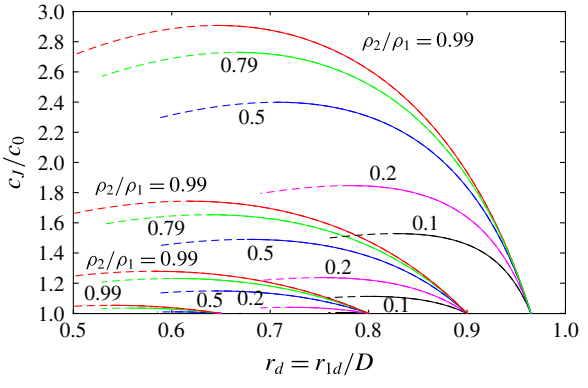

FIGURE 5. (Colour online) Hydraulic jump (hydraulic drop) speeds c_J scaled with c_0 as in figure 4 for $r_u = 0.65$, 0.8, 0.9 and 0.965. Amplitudes greater than those for maximum speed are shown dashed.

In each case, the point of the double maximum coincides with the maximum in the jump speed, and the speed curves in figures 4 and 5 are terminated at the point of zero loss of energy flux.

The termination point represents a transition through the jump to a two-layer flow state with the same energy fluxes in each layer (and zero loss through the jump), which is described as a flow state that is 'conjugate' to the original upstream state (Benjamin 1966; Lamb & Wan 1998). Solutions of (3.8) and (3.12) for larger amplitudes are possible but are essentially unphysical, since they would require a gain in energy flux within the jump. Hence the conjugate flow state represents the maximum jump amplitude.

The criterion for maximum speed of the hydraulic jump coincides (or very nearly coincides) with another property, namely that where the flow downstream of the jump becomes critical, in the frame of the jump. Figure 7 shows a representative example of this for $r_u = 0.1$, where the upper curves show the jump speeds, and the lower dashed curves the speeds of leftward-propagating waves (relative to the jump) on the downstream side. The zeros for these downstream wave speeds occur at r_d values very

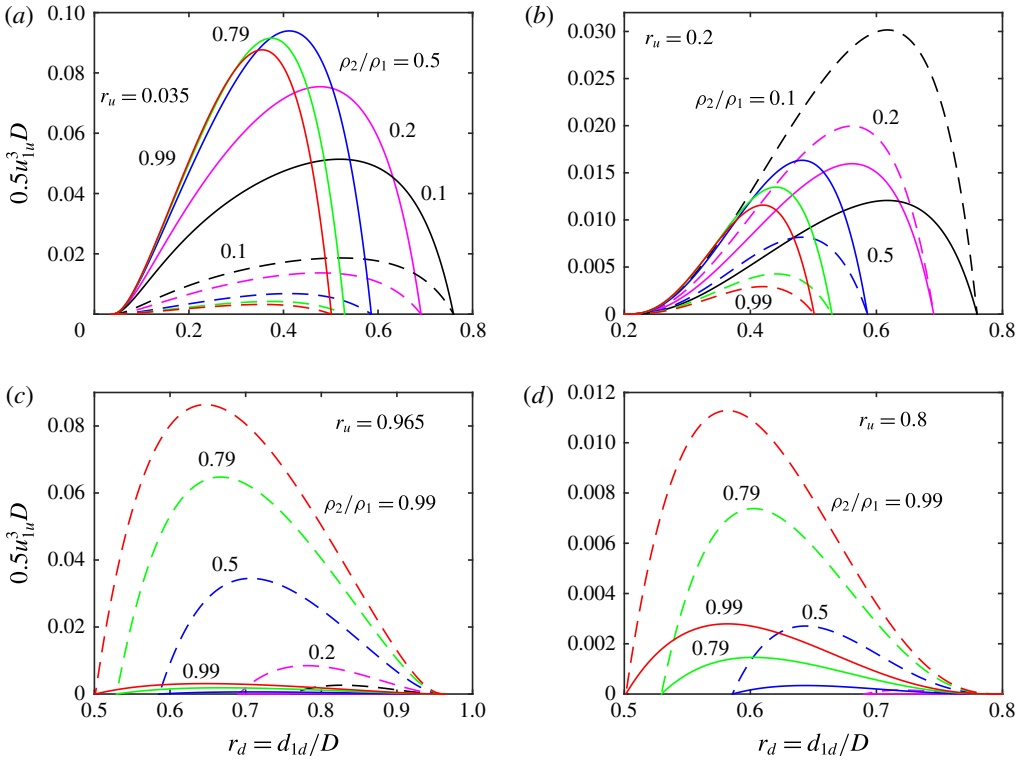

FIGURE 6. (Colour online) Energy flux losses for each layer within the hydraulic jump for (*a*) $r_u = 0.035$, (*b*) $r_u = 0.2$, (*c*) $r_u = 0.965$ and (*d*) $r_u = 0.8$, for $\rho_2/\rho_1 = 0.1$, 0.2, 0.5, 0.79 and 0.99. The solid lines denote the upper layer, the dashed lines the lower layer. Note that the upper layer is contracting in (*a*,*b*), but the lower layer is contracting in (*c*,*d*), which show results for hydraulic drops.

slightly smaller (∼0.1 %) than those for maximum jump speed. Similar diagrams can be derived for other r_u values. This means that, for jump amplitudes smaller than that for maximum speed, disturbances downstream of the jump are able to propagate up to the jump, and potentially affect it by increasing or decreasing its amplitude. For larger jump amplitudes with lower jump speeds, the downstream flow is supercritical (relative to the jump), and disturbances from downstream cannot propagate to the jump and influence it. This means, in particular, that jumps with amplitudes larger than jumps with maximum speed cannot be created by forcing from downstream, whereas smaller-amplitude jumps can. This applies to upstream jumps that are forced by flow over topography either by a slow increase in the flow or by an obstacle of slowly increasing height. This implies that it may be difficult to realise these larger-amplitude jumps.

Further, if jumps with magnitudes greater than that for maximum jump speed (and dissipation) are formed, they are probably unstable. This is because, if the amplitude of the leading part of such a jump is decreased slightly, it will travel faster, and the larger-amplitude component will lag behind. Conversely, an increase in the jump amplitude will cause it to travel more slowly, and again the highest part will lag behind. For these two reasons – difficulty of generation and inherent instability – the practical relevance of the jumps with speeds greater than the maximum is

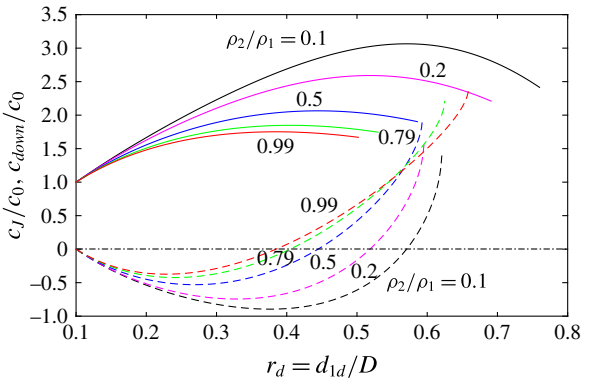

FIGURE 7. (Colour online) Hydraulic jump speeds c_J scaled with c_0 as in figures 2 and 4 for $r_u = 0.1$, together with (leftward-propagating) linear wave speeds (in the frame of the jump) on the downstream side. The flow is subcritical (wave speeds are negative, towards the jump) for jump heights less than the value for maximum speed, and supercritical (wave speeds are positive) for jump heights greater than this value.

doubtful, although, like the conjugate states, there may be special situations where they may be formed and sustained. Dam-break flows are one situation in which the large-amplitude jumps may be formed, but they would then be subject to the instability that would lead to a jump of maximum speed followed by a wave field. Numerical results by White & Helfrich (2014) of jumps formed (by dam-break) in Boussinesq near-two-layer continuous stratification show maximum jump amplitude coinciding with maximum jump speed and zero energy loss for $r_u = 0.1$ and 0.2, but not for 0.4. There is scope for further work to resolve these details.

In figure 6, (*a*,*b*) are for hydraulic jumps and (*c*,*d*) are for hydraulic drops. The energy flux losses (notionally due to turbulent dissipation) show that, if the densities of the two layers are comparable, most of the energy flux is lost in the contracting layer. As the relative density of the upper layer decreases, the energy flux loss there decreases in proportion, as may be seen in figure 6(*b*). In (*c*,*d*), the contracting lower layer dominates the energy flux loss regardless of the density difference. As $\rho_2/\rho_1 \to 1$ in (*a*,*b*) the energy loss of the lower layer becomes small but not zero: the dissipation rates shown for $\rho_2/\rho_1 = 0.99$ are very close to the limiting values ($\rho_2/\rho_1 = 0.999$ gives the same result). This provides some justification for the KRS approximation and Borden and Meiburg's VS Boussinesq model when ρ_2/ρ_1 is close to unity, but the results are not precise. For larger r_u, relatively more dissipation occurs in the lower layer: for $r_u = 0.2$, the changeover occurs near $\rho_2/\rho_1 = 0.25$.

5. Profiles with a diffuse or mixing interface

In their study of Boussinesq internal bores, Borden and Meiburg extended their model to include a mixing layer between the two fluids by assuming a linear variation in both the density and velocity in place of a sharp interface. This may also be done here for the general case, but of course it only applies if the fluids are miscible. There are several options. One may regard the mixing as a process occurring within the hydraulic jump with an upstream two-layer flow as described above and a downstream flow with a mixed layer. Alternatively, one may also have a mixed layer in the upstream flow, whether or not the velocities in the two layers are the same. The analysis below covers both of these cases.

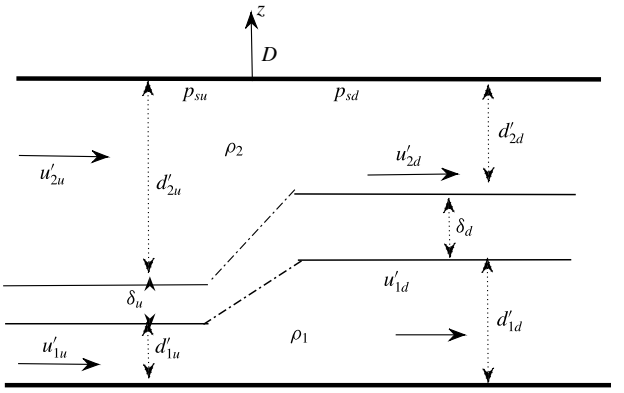

FIGURE 8. Definition sketch (similar to figure 1) for a hydraulic jump with a linear transition region between the upper and lower layers, both upstream and downstream. Velocities are given in the frame of the jump.

We consider the general case with jump structure as shown in figure 8, with a linear transition in both density and velocity between the upper and lower layers, both upstream and downstream. The notation is the same as in figure 1, except for the additional layer and the fact that the velocities and thicknesses of the upper and lower layers are denoted by dashes, to distinguish them from the case of figure 1. The central layer has the thickness δ_u upstream and δ_d downstream, and if z^* is the vertical coordinate within the central layer the velocity and density there (in a frame of reference moving with the jump) have the form

$$u(z^*) = u'_{1u} + \frac{z^*}{\delta_u}(u'_{2u} - u'_{1u}), \quad \rho(z^*) = \rho_1 - \frac{z^*}{\delta_u}(\rho_1 - \rho_2), \quad 0 < z^* < \delta_u, \tag{5.1a,b}$$

$$u(z^*) = u'_{1d} + \frac{z^*}{\delta_d}(u'_{2d} - u'_{1d}), \quad \rho(z^*) = \rho_1 - \frac{z^*}{\delta_d}(\rho_1 - \rho_2), \quad 0 < z^* < \delta_d, \tag{5.2a,b}$$

where the first equation applies upstream and the second downstream. We also have

$$d'_{1u} + d'_{2u} + \delta_u = D, \quad d'_{1d} + d'_{2d} + \delta_d = D. \tag{5.3a,b}$$

As before, our objective is to obtain expressions for the flow downstream of the jump in terms of the flow properties upstream. Since the fluids are incompressible, volume conservation gives the equation

$$u'_{1u}d'_{1u} + u'_{2u}d'_{2u} + (u'_{1u} + u'_{2u})\frac{\delta_u}{2} = u'_{1d}d'_{1d} + u'_{2d}d'_{2d} + (u'_{1d} + u'_{2d})\frac{\delta_d}{2}, \tag{5.4}$$

and similarly mass conservation gives

$$\begin{aligned} u'_{1u}d'_{1u} + \frac{\rho_2}{\rho_1}u'_{1u}d'_{1u} + \frac{\delta_u}{6}\left[u'_{1u}\left(2 + \frac{\rho_2}{\rho_1}\right) + u'_{2u}\left(1 + 2\frac{\rho_2}{\rho_1}\right)\right] \\ = u'_{1d}d'_{1d} + \frac{\rho_2}{\rho_1}u'_{1d}d'_{1d} + \frac{\delta_d}{6}\left[u'_{1d}\left(2 + \frac{\rho_2}{\rho_1}\right) + u'_{2d}\left(1 + 2\frac{\rho_2}{\rho_1}\right)\right]. \end{aligned} \tag{5.5}$$

The remaining equation is the conservation of momentum flux (2.2); inserting the hydrostatic pressure as before, one obtains for the downstream side

$$S = \frac{1}{2}\rho_2 g d^2 + p_{sd} + \frac{1}{6}g(\rho_1 - \rho_2)[(D - d'_{2d})^2 + d'_{1d}(D - d'_{2d}) + d'^2_{2d}] + \rho_1 d'_{1d}u'^2_{1d} + \rho_2 d'_{2d}u'^2_{2d} + \frac{\delta_d}{12}[u'^2_{1d}(3\rho_1 + \rho_2) + u'^2_{2d}(\rho_1 + 3\rho_2) + 2u'_{1d}u'_{2d}(\rho_1 + \rho_2)], \tag{5.6}$$

which is equal to the corresponding expression (with subscript 'u' replacing subscript 'd') on the upstream side.

As before, we need an expression for the difference in surface pressure $p_{su} - p_{sd}$, and this is again obtained from the vorticity balance which, in the same manner as in § 3, yields

$$\frac{\Delta\rho}{\rho_1}\frac{p_{su} - p_{sd}}{\rho_2} = \frac{1}{2}(u'^2_{2d} - u'^2_{1d}) - \frac{1}{2}(u'^2_{2u} - u'^2_{1u}) - \frac{\Delta\rho g}{\rho_1}(d'_{1d} - d'_{2d} - d'_{1u} + d'_{2u}). \tag{5.7}$$

Substituting this into (5.5) gives the fourth equation for the downstream flow. If δ_d and δ_u have prescribed values, (5.2)–(5.6) may be solved numerically to determine the jump speed and downstream conditions in terms of those upstream, as in § 3.

It remains to determine appropriate values of the intermediate layer thickness, δ_d and δ_u. The value of δ_u will be dependent on processes upstream of the jump, and we assume it to be zero here. If we restrict consideration to the case where the upstream flow has uniform speed with no mixing layer (i.e. $\delta_u = 0$, with $u_{2u} = u_{1u}$), for miscible fluids the thickness δ_d will be determined by mixing processes within the jump. In a general sense, these may be related to shear instability within the jump, which is governed by the Richardson number R_i, defined by $R_i = N^2/(\mathrm{d}u/\mathrm{d}z)^2$, where the buoyancy frequency N is given by $N^2 = -(g/\rho)\mathrm{d}\rho/\mathrm{d}z$. On the downstream side of the jump, this gives

$$R_i(z^*) = \frac{\rho_1 - \rho_2}{(u'_{2d} - u'_{1d})^2\left(\rho_1 - \dfrac{z^*}{\delta_d}(\rho_1 - \rho_2)\right)}, \tag{5.8}$$

which has maximum and minimum values at the top and bottom (respectively) of the central layer, with values

$$R_{imax} = \frac{\Delta\rho g\delta_d}{\rho_2(u'_{2d} - u'_{1d})^2}, \quad R_{imin} = \frac{\Delta\rho g\delta_d}{\rho_1(u'_{2d} - u'_{1d})^2}. \tag{5.9a,b}$$

If $R_i > 1/4$ in a density-stratified shear flow, internal waves may propagate through it, but if $R_i < 1/4$ they cannot. The instability of this shear layer depends on the mutual interaction of waves propagating on the vorticity interfaces at the top and bottom of the layer, and wave propagation in the fluid between them disrupts this process. Hence, if $R_{imin} > 1/4$ the flow will be stable, but if $R_{imax} < 1/4$ it will be unstable. Here we base the value of δ_d on the second criterion, and obtain

$$\Delta_d = \delta_d/D = \frac{\rho_2(u'_{2d} - u'_{1d})^2}{\Delta\rho g D}. \tag{5.10}$$

(This choice is, to some extent, arbitrary, and may underestimate δ_d, but the scaling is robust.) To compute these values numerically for increasing values of $r'_d = d'_{1d}/D$, one

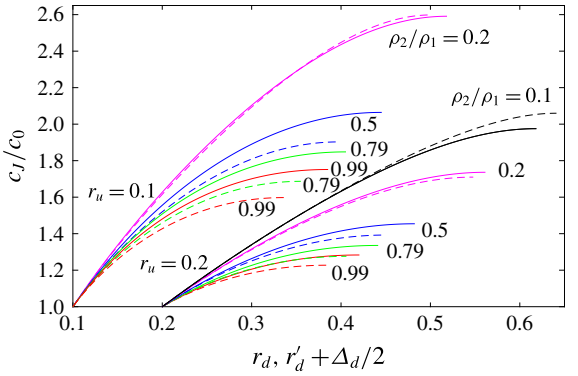

FIGURE 9. (Colour online) Comparisons of jump speeds between flows without a mixed transition layer, as previously (solid curves), and flows with a downstream transition layer (dashed curves) with thickness derived via (5.10), for some representative cases. The abscissa is r_d for the solid curves, $r'_d+\Delta_d/2$ for the dashed curves.

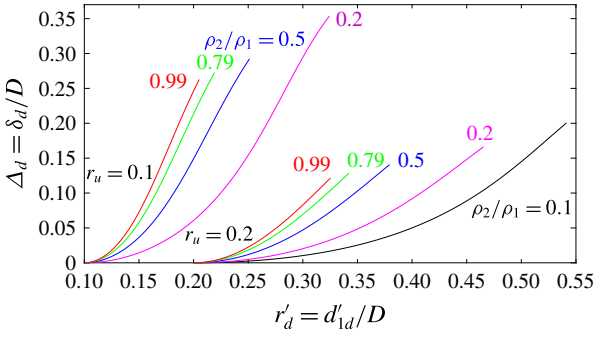

FIGURE 10. (Colour online) The thickness $\Delta_d=\delta_d/D$ obtained from (5.10) for the cases with jump speeds as given in figure 9.

takes $\delta_d=0$ for the initial increment and uses the values from the previous increment to give the next value of δ_d; the error involved is negligible if the increments are sufficiently small.

Some representative results from such calculations are shown in figures 9 and 10. Figure 9 shows comparisons between jump speeds for $r_u=0.1$ and 0.2 between cases with no (partially) mixed layer (solid lines) and flows with a downstream mixed layer (dashed curves) as defined in (5.10). Here the jump speeds with mixing are less than those without, except when ρ_2/ρ_1 is small. Thicknesses of the mixed layer for the same parameter values are shown in figure 10. It is seen that, even with the conservative estimate of (5.10), the transition layer thickness becomes quite substantial with increasing jump amplitude.

6. Conclusions

I have described a new model for the properties of hydraulic jumps between two uniform states of two-layer flow, covering the complete range of densities from a single layer to the Boussinesq limit. The procedure is an extension of the VS model of Borden & Meiburg (2013), and is based on the generation of vorticity within the

jump, as determined by the differing upstream and downstream flows. Unlike previous models, it does not require any assumptions about the internal dynamics (hydrostatic flow in YG) or energy losses within the jump (CBWS, KRS), and may be termed the full vortex sheet (FVS) model. The main point is that the vorticity produced by the jump is contained in the downstream flow: its generation depends only on the pressure field across the jump, which is determined from (3.2).

This model is consistent with all the expected limits, and is in good agreement with experimental observations of jump speeds, over a range of parameters for which comparisons can be made (Baines 1984). Energy dissipation (or energy flux loss) within the jump is always positive for each layer, and is largest for the contracting layer, except when it is the upper layer and the density of the latter is relatively small. Maximum energy loss in each layer coincides with maximum jump speeds. For jumps with amplitudes larger than that of maximum speed, the energy losses of both layers decrease with increasing amplitude, to the limit of the 'conjugate state' of zero energy loss.

The flow downstream of a jump is subcritical (in the frame of the jump) for jump amplitudes less than that for maximum speed, which means that waves from downstream may approach and influence the jump. For jumps with larger amplitude, the lee-side flow is supercritical and downstream waves cannot approach it (the critical condition does not coincide with the maximum speed, but occurs very slightly before it). This has implications for jumps formed upstream of topography, for example. Further, it is argued that the jumps with amplitudes larger than that for maximum speed are unstable, since a small decrease in their height will cause them to travel faster.

If the fluids in the two layers are immiscible, mixing between them cannot occur. But if they are miscible, then a mixing layer may form downstream of the jump, with (approximately) linear profiles in density and velocity. Such mixing is governed by shear instability and the Richardson number in the central layer. Equations governing this situation are presented, with some representative results for downstream conditions and central layer thicknesses.

Acknowledgement

The author is grateful to E. Meiburg for helpful comments on an early version of this manuscript, including pointing out the simplification obtained using Stokes's theorem.

REFERENCES

BAINES, P. G. 1984 A unified description of two-layer flow over topography. *J. Fluid Mech.* **146**, 127–167.

BAINES, P. G. 1995, 1997 *Topographic Effects in Stratified Flows*. Cambridge University Press.

BENJAMIN, T. B. 1966 Internal waves of finite amplitude and permanent form. *J. Fluid Mech.* **25**, 241–270.

BENJAMIN, T. B. 1968 Gravity currents and related phenomena. *J. Fluid Mech.* **31**, 209–248.

BORDEN, Z. & MEIBURG, E. 2013 Circulation-based models of Boussinesq internal bores. *J. Fluid Mech.* **276**, R1.

BORDEN, Z., MEIBURG, E. & CONSTANTINESCU, G. 2012 Internal bores: an improved model via a detailed analysis of the energy budget. *J. Fluid Mech.* **703**, 279–314.

CHU, V. H. & BADDOUR, R. E. 1977 Surges, waves and mixing in two-layer density stratified flow. In *Proceedings of the 17th International Association of Hydraul. Res.*, vol. 1, pp. 303–310. IAHR.

KLEMP, J. B., ROTUNNO, R. & SKAMAROCK, W. C. 1997 On the propagation of internal bores. *J. Fluid Mech.* **331**, 81–106.

LAMB, K. G. & WAN, B. 1998 Conjugate flows and flat solitary waves for a continuously stratified fluid. *Phys. Fluids* **10**, 2061–2069.

LI, M. & CUMMINS, P. F. 1998 A note on hydraulic theory of internal bores. *Dyn. Atmos. Oceans* **28**, 1–7.

SAFFMAN, P. G. 1992, 1995 *Vortex Dynamics*. Cambridge University Press.

THORPE, S. A. 2010 Turbulent hydraulic jumps in a stratified shear flow. *J. Fluid Mech.* **654**, 305–350.

THORPE, S. A. & LI, LIN 2014 Turbulent hydraulic jumps in a stratified shear flow. Part 2. *J. Fluid Mech.* **758**, 94–120.

WHITE, B. L. & HELFRICH, K. R. 2014 A model for internal bores in continuous stratification. *J. Fluid Mech.* **761**, 282–304.

WOOD, I. R. & SIMPSON, J. E. 1984 Jumps in layered miscible fluids. *J. Fluid Mech.* **140**, 329–342.

YIH, C.-S. & GUHA, C. R. 1955 Hydraulic jump in a fluid system of two layers. *Tellus* **7**, 358–366.